European Journal of Nuclear Medicine and Molecular Imaging
https://doi.org/10.1007/s00259-018-3965-8

ORIGINAL ARTICLE

Tracer uptake in mediastinal and paraaortal thoracic lymph nodes as a potential pitfall in image interpretation of PSMA ligand PET/CT

Ali Afshar-Oromieh[1,2] · Lars Peter Sattler[1] · Katja Steiger[3] · Tim Holland-Letz[4] · Marcelo Livorsi da Cunha[5] · Walter Mier[1] · Oliver Neels[6,7] · Klaus Kopka[6,7] · Wilko Weichert[3,8] · Uwe Haberkorn[1,2]

Received: 13 November 2017 / Accepted: 25 January 2018

Abstract

Purpose Since the introduction of ^{68}Ga-PSMA-11 PET/CT for imaging prostate cancer (PC) we have frequently observed mediastinal lymph nodes (LN) showing tracer uptake despite being classified as benign. The aim of this evaluation was to further analyze such LN.

Methods Two patient groups with biphasic ^{68}Ga-PSMA-11 PET/CT at 1 h and 3 h p.i. were included in this retrospective evaluation. Group A ($n = 38$) included patients without LN metastases, and group B ($n = 43$) patients with LN metastases of PC. SUV of mediastinal/paraaortal LN of group A ($n = 100$) were compared to SUV of LN metastases of group B ($n = 91$). Additionally, 22 randomly selected mediastinal and paraaortal LN of patients without PC were immunohistochemically (IHC) analyzed for PSMA expression.

Results In group A, 7/38 patients (18.4%) presented with at least one PSMA-positive mediastinal LN at 1 h p.i. and 3/38 (7.9%) positive LN at 3 h p.i. with a SUVmax of 2.3 ± 0.7 at 1 h p.i. (2.0 ± 0.7 at 3 h p.i.). A total of 11 PSMA-positive mediastinal/paraaortal LN were detected in nine patients considering both imaging timing points. SUVmax of LN-metastases was 12.5 ± 13.2 at 1 h p.i. (15.8 ± 17.0 at 3 h p.i.). SUVmax increased clearly (> 10%) between 1 h and 3 h p.i. in 76.9% of the LN metastases, and decreased significantly in 72.7% of the mediastinal/paraaortal LN. By IHC, PSMA-expression was observed in intranodal vascular endothelia of all investigated LN groups and to differing degrees within germinal centers of 15/22 of them (68.1%). Expression was stronger in mediastinal nodes ($p = 0.038$) and when follicular hyperplasia was present ($p = 0.050$).

Conclusion PSMA-positive mediastinal/paraaortal benign LN were visible in a notable proportion of patients. PSMA-positivity on the histopathological level was associated with the activation state of the LN. However, in contrast to LN metastases of PC, they presented with significantly lower uptake, which, in addition, usually decreased over time.

Keywords Prostate cancer · PET/CT · Mediastinal · Mediastinal/paraaortal · Lymph nodes · PSMA · Prostate-specific membrane antigen · ^{68}Ga-PSMA-11

Introduction

Prostate cancer (PC) is the most prevalent tumor entity in men worldwide [1]. After initial therapy, biochemical recurrence is frequent in patients with high-risk PC. Detection of recurrent PC has always been challenging for computed tomography (CT), magnetic resonance imaging (MRI), and other conventional imaging modalities.

✉ Ali Afshar-Oromieh
a.afshar@gmx.de

[1] Department of Nuclear Medicine, Heidelberg University Hospital, INF 400, 69120 Heidelberg, Germany

[2] Department of Nuclear Medicine, Bern University Hospital (Inselspital), Bern, Switzerland

[3] Institute of Pathology, Technical University of Munich, Munich, Germany

[4] Department of Biostatistics, German Cancer Research Center, Heidelberg, Germany

[5] Department of Nuclear Medicine, Hospital Israelita Albert-Einstein, São Paulo, Brazil

[6] Division of Radiopharmaceutical Chemistry, German Cancer Research Center, Heidelberg, Germany

[7] German Cancer Consortium (DKTK), Heidelberg, Germany

[8] German Cancer Consortium (DKTK), Munich, Germany

Published online: 01 March 2018

In recent years, the prostate-specific membrane antigen (PSMA), also known as folate hydrolase I or glutamate carboxypeptidase II, has moved into focus of attention as an excellent target for, both, imaging and therapy of PC. PSMA is considered to be the most well established target antigen in PC, since it is strongly expressed on the surface of PC cells [2].

Following multiple years of substantial preclinical research, the first human experience in PSMA-ligand imaging was published in 2008–2009 using ^{123}I–MIP-1072 and ^{123}I–MIP-1095 [3, 4]. The clinical breakthrough and spread followed in 2011 with the introduction of ^{68}Ga-PSMA-11 for PET-imaging and ^{131}I–MIP-1095 for PSMA-ligand therapy of metastatic PC [5–11].

Despite its name, PSMA is not specific for prostate cancer. Since the late 1990s, it has been known that the neovasculature of many solid tumors expresses PSMA as well [12]. Since the introduction of PET imaging with ^{68}Ga-PSMA-11, many reports have been published showing various non-prostatic tissues of benign and malign origin presenting with an uptake of PSMA ligands [13]. The biodistribution of ^{68}Ga-PSMA-11 and of alternative PSMA ligands shows physiological uptake in the lacrimal and salivary glands, in the liver, in the spleen, in the kidneys, in some parts of the intestines, and in coeliac ganglia [5, 14]. In addition, we frequently observed a tracer uptake in mediastinal or paraaortal thoracic lymph nodes (LN). Although the tracer uptake in such LN is usually low, a clear differentiation to LN-metastases of PC with low tracer uptake can be challenging in some cases.

To our knowledge, an observation and analysis of PSMA-positive mediastinal/paraaortal LN has never been published before. The aim of this evaluation was to further analyze both the histological and imaging characteristics of mediastinal/paraaortal LN and to compare them to LN metastases of PC.

Materials and methods

Patients

Characteristics of all patients included in this retrospective analysis are summarized in Table 1. The majority of the patients have been analyzed in several previous studies addressing different topics [5–7, 9, 15].

Patient selection criteria are presented in Fig. 1. Out of all patients who were referred to ^{68}Ga-PSMA-11 PET/CT between May 2011 and May 2017 (n = 1492) at our department in order to detect PC, 81 received a biphasic scan at 1 h (h) and 3 h p.i. including at least pelvis, abdomen, and thorax.

Amongst the 81 above-mentioned patients, 38 presented without evidence of LN metastases and were therefore referred to group A. Group A therefore also included patients without a pathologic scan. The mentioned inclusion criteria were chosen in order to minimize the probability of mediastinal LN metastases of PC.

Forty-three of the above-mentioned 81 patients presented with at least one lesion suggestive of LN-metastasis of PC, and were referred to group B.

Radiotracer

^{68}Ga-PSMA-11 was produced as previously described [7, 16]. Briefly, [^{68}Ga]Ga^{3+} was obtained from a ^{68}Ge/^{68}Ga radionuclide generator and used for radiolabeling of PSMA-11. The ^{68}Ga-PSMA-11 solution was applied to the patients via an intravenous bolus injection (mean of 153.8 ± 76.5 MBq, range 40–345 MBq). The targeted injected activity was 2 MBq per kilogram body weight. Variation of injected radiotracer activity was caused by the short physical half-life of ^{68}Ga (68 min), variable elution efficiencies resulting during the lifetime of the ^{68}Ge/^{68}Ga generator, and unexpected delays in clinical routine.

Imaging

The imaging procedure and scanning protocol is equivalent to our previous study to which we hereby refer [9]. Briefly, the patients of this evaluation were investigated with two different scanners. A Biograph-6 PET/CT scanner was used until August 2015 and was then replaced by a Biograph mCT Flow scanner (both scanners made by Siemens, Erlangen, Germany). The two different PET/CT scanners were cross-calibrated.

With regard to the Biograph-6 PET/CT, the scan protocol (1 h p.i.: whole body and 3 h p.i.: whole body or part body) was as described previously [7]. With regard to the Biograph mCT Flow scanner, a non-contrast-enhanced whole-body CT scan

Table 1 Characteristics of patients analyzed in this evaluation

	Age (years)	Trace (MBq)	GSC	PSA at PET (ng/ml)
Mean	72.1	153.8	7.6	10.36
SD	8.2	76.5	1.1	25.99
Range	43–90	40–345	5–10	0.01–176.00
Median	73.0	135.0	7.0	4.51
Prostatectomy	Radiation therapy	ADT	chemotherapy	Primary staging
66	54	37	7	3

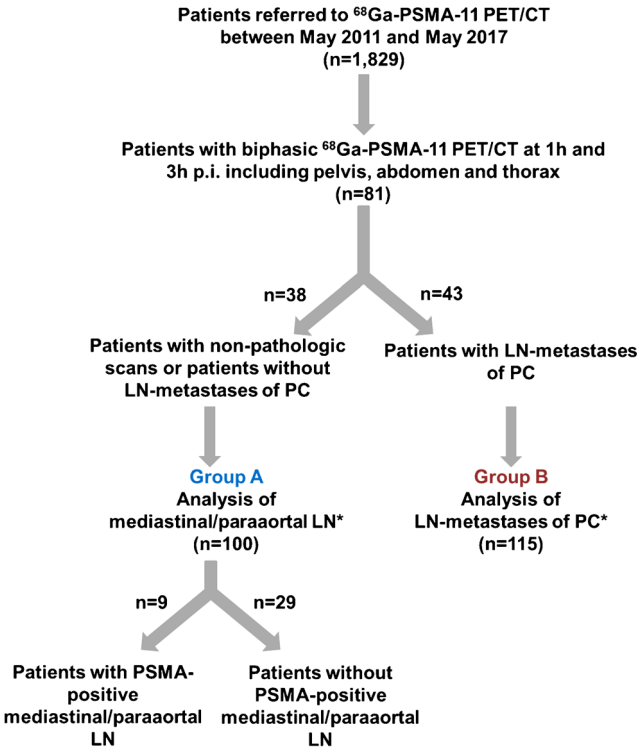

Fig. 1 Inclusion criteria of patients. * A maximum of five mediastinal/paraaortal or metastatic LN per patient were randomly selected and analyzed in this evaluation

was performed at 1 h p.i. using the following parameters: slice thickness of 5 mm, increment of 3–4 mm, soft-tissue reconstruction kernel, care dose. Immediately after CT scanning, a PET scan was acquired in 3-D (matrix 200 × 200) in flow motion with 0.7 cm/min. The emission data were corrected for randoms, scatter, and decay. Reconstruction was conducted with an ordered subset expectation maximization (OSEM) algorithm with two iterations/21 subsets, and Gauss-filtered to a transaxial resolution of 5 mm at full width at half maximum (FWHM). Attenuation correction was performed using the low-dose non-enhanced CT data. PET and CT were performed using the same protocol for every patient on a Biograph mCT Flow scanner (Siemens, Erlangen, Germany).

Lesion evaluation

Two physicians, board certified in nuclear medicine with 13 and 7 years of clinical experience (first and second author), evaluated all data sets together and resolved any disagreements by consensus. Any uptake of ^{68}Ga-PSMA-11 above local background in CT-morphologically visible lesions was considered as PSMA-positive. The classification of benign or malignant origin of the lesions was conducted in the clinical context by the above-mentioned authors.

Group A: mediastinal and paraaortal LN which were visually considered as PSMA-positive and of benign origin were counted and analyzed with respect to their mean and maximum standardized uptake value (SUVmean and SUVmax) at 1 h and 3 h p.i.. The same procedure was conducted for PSMA-negative mediastinal/paraaortal LN for up to a maximum of five representative LN per patient. Due to the latter procedure, an independent reading of the data-set by the two above-mentioned readers was not suitable.

Group B: lesions that were visually considered as suggestive of LN metastases of PC were also counted up to a maximum number of five per patient and analyzed in the same way as LN of group A. This kind of selection (maximum number of five selected LN metastases) significantly reduces an overestimation of SUV values, as otherwise dominant lesions could be preferentially selected.

SUV values of the same lesions at both 1 h and 3 h p.i. were defined as clearly less, equal, or clearly more with intensity differences of ≤ 10%, between −10 and +10%, or > 10% respectively.

Histology and immunohistochemistry

Twenty-two lymph node samples (some of them including several nodes) from 22 distinct patients who were surgically treated for cancer diseases other than PC were investigated. Patients with history of PC were excluded to avoid any potential confounding factor such as, for example, tumor-borne soluble PSMA deposited in such nodes. The investigation was approved by the local ethics committee (5549/12).

Eleven node samples were from the mediastinum, 11 were from paraaortal regions. None of the nodes showed any tumor seeding. All nodes were evaluated with respect to histopathological alterations on hematoxylin and eosin (H&E) sections. On consecutive slides, immunohistochemistry for PSMA was performed with a Bond RXm system (Leica, Wetzlar, Germany, all reagents from Leica) with a primary antibody against PSMA (Abcam, Cambridge, UK, clone EPR6253 diluted 1:100 in antibody diluent). Briefly, slides were deparaffinized using deparaffinization solution, and pretreated with Epitope retrieval solution 1 (corresponding to citrate buffer pH 6) for 20 min. Antibody binding was detected with a polymer refine detection kit without post primary reagent and visualized with diaminobenzidine as a dark brown precipitate. Counterstaining was done with hematoxyline.

Staining of endothelial cells both in vessel walls and in germinal centers (the only two positive structural elements observed) were semiquantitatively evaluated as being not present, weak, moderate, or strong by a board-certified pathologist (WW).

Statistical analysis

Significance of SUV differences between PSMA-negative and PSMA-positive mediastinal/paraaortal LN as well as between PSMA-positive mediastinal/paraaortal LN and LN

metastases of PC at both imaging timings (1 h and 3 h p.i.) was evaluated using a linear mixed model including the patient-ID as a random factor by using paired *t*-tests (Package lme4 of the R version 3.4.0 software). Thus, possible effects of having multiple LNs per patient were accounted for. A p value of < 0.05 was considered statistically significant.

Differences in immunhistologically determined PSMA positivity scores (0 to 3) in both vessels and germinal centers were compared for different pathologies (no pathology, fibrosis, focal hyperplasia, diffuse hyperplasia) and site (paraaortal/mediastinal) using unpaired Wilcoxon's tests. Association of pathologies with site were compared with Fishers exact test. A p value of < 0.05 was considered statistically significant. All tests were performed as two-sided tests.

Results

Group A

Within group A (patients without evidence of LN metastases), a total number of 100 mediastinal/paraaortal LN were evaluated in 38 patients. At 1 h p.i., eight LN in seven of the 38 patients (18.4%) presented with a visually positive PSMA-ligand uptake such as presented by Figs. 2 and 3 (one patient with two PSMA-positive LN). At 3 h p.i., three PSMA-positive LN were detected in three patients (7.9%) as presented by Figs. 4 and 5. Subsequently, a total of 11 PSMA-positive mediastinal/paraaortal LN were detected in nine patients considering both imaging time points.

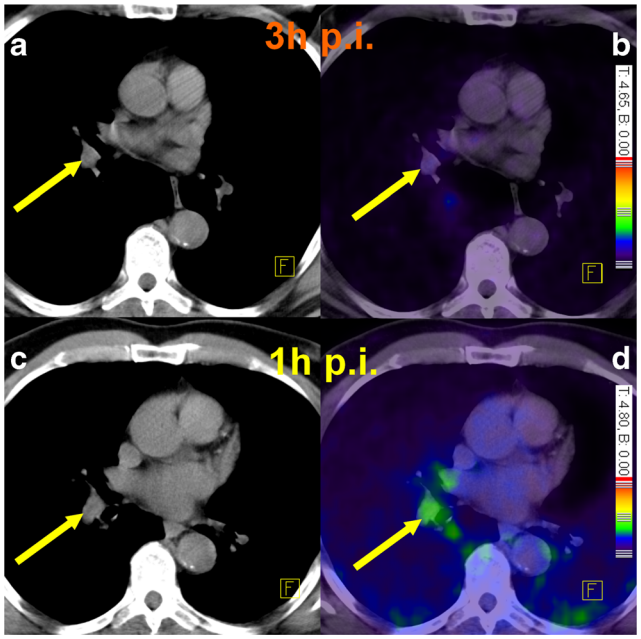

Fig. 3 An example of a hilar, slightly PSMA-positive LN (*yellow arrows*) at 1 h p.i. with a SUVmax of 2.1, which turned to PSMA-negative at 3 h p.i. (SUVmax 0.9). **a** Low-dose CT at 3 h p.i. **b** fusion of PET and CT at 3 h p.i. **c** Low-dose CT at 1 h p.i. **d** Fusion of PET and CT at 1 h p.i. Color scales as automatically produced by the PET/CT scanner

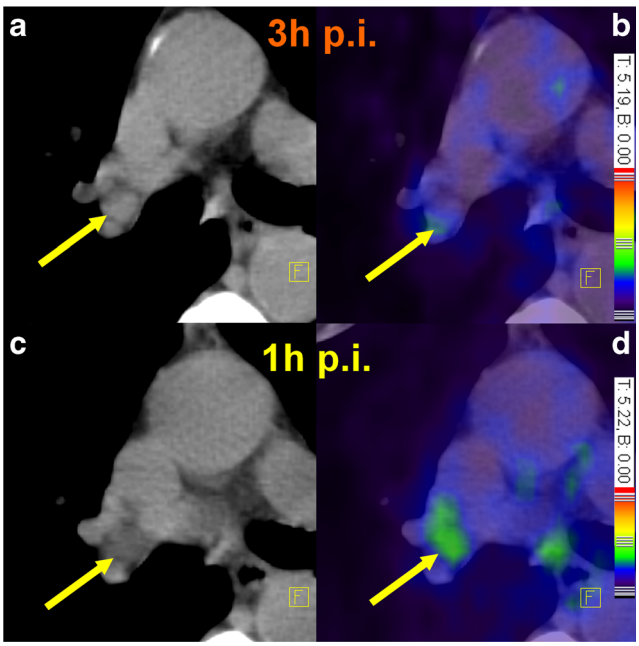

Fig. 2 *Yellow arrows* point to a mediastinal, slightly PSMA-positive LN at 1 h p.i. (SUVmax 2.0), which turned to PSMA-negative at 3 h p.i. (SUVmax 1.2). **a** Low-dose CT at 3 h p.i. **b** Fusion of PET and CT at 3 h p.i. **c** Low-dose CT at 1 h p.i. **d** fusion of PET and CT at 1 h p.i. Color scales as automatically produced by the PET/CT scanner

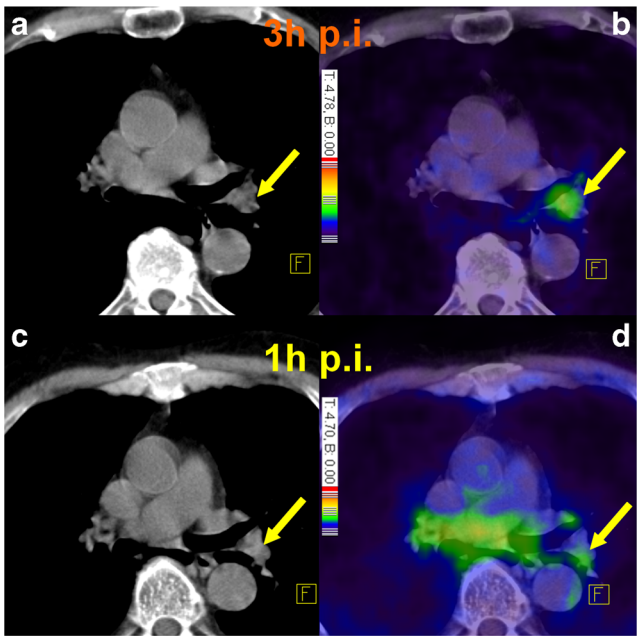

Fig. 4 *Yellow arrows* point to a hilar, PSMA-negative LN at 1 h p.i. (SUVmax 2.1), which turned to PSMA-positive at 3 h p.i. (SUVmax 2.7). **a** Low-dose CT at 3 h p.i. **b** Fusion of PET and CT at 3 h p.i. **c** Low-dose CT at 1 h p.i. **d** Fusion of PET and CT at 1 h p.i. Color scales as automatically produced by the PET/CT scanner

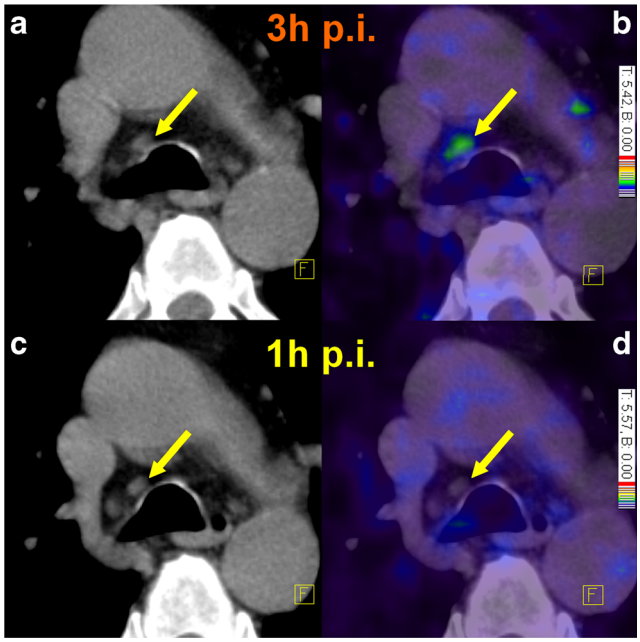

Fig. 5 An example of a mediastinal, PSMA-negative LN (*yellow arrows*) at 1 h p.i. (SUVmax 0.5), which turned to PSMA-positive at 3 h p.i. (SUVmax 2.7). **a** Low-dose CT at 3 h p.i. **b** Fusion of PET and CT at 3 h p.i. **c** Low-dose CT at 1 h p.i. **d** Fusion of PET and CT at 1 h p.i. Color scales as automatically produced by the PET/CT scanner

With regard to PSMA-negative mediastinal/paraaortal LN ($n = 89$), SUVmean was 1.0 ± 0.3 (range 0.1–1.9; median 1.0) at 1 h p.i. and 0.8 ± 0.3 (range 0.2–1.9; median 0.7) at 3 h p.i.. SUVmax was 1.2 ± 0.5 (0.2–2.8; median 1.2) at 1 h p.i. and 0.9 ± 0.4 (range 0.3–2.4; median 0.9) at 3 h p.i..

SUVmean of PSMA-negative mediastinal/paraaortal LN clearly (>10%) increased in seven (7.9%) lesions, clearly decreased in 67 (75.3%) lesions, and remained stable in 15 (16.9%) of the LN between 1 and 3 h p.i..

SUVmax of PSMA-negative mediastinal/paraaortal LN clearly (>10%) increased in eight (9.0%) lesions, clearly decreased in 67 (75.3%) lesions, and remained stable in 14 (15.7%) of the LN between 1 and 3 h p.i..

As presented by Fig. 6, PSMA-positive mediastinal/paraaortal LN presented with a SUVmean of 1.8 ± 0.5 (range 0.4–2.4; median 1.8) at 1 h p.i. and 1.4 ± 0.6 (range 0.7–2.5; median 1.3) at 3 h p.i.. SUVmax was 2.3 ± 0.7 (range 0.5–3.2; median 2.4) at 1 h p.i. and 2.0 ± 0.7 (range 0.9–3.4; median 1.9) at 3 h p.i..

Both SUVmean and SUVmax clearly (> 10%) increased in three PSMA-positive mediastinal/paraaortal LN (27.3%), clearly decreased in eight LN (72.7%) and remained stable in zero (0%) LN between 1 and 3 h p.i.

Group B

Within group B (patients with LN metastases of PC), a total number of 91 LN suggestive of PC metastases were evaluated. As presented by Fig. 2, the SUVmean of them was 6.6 ± 6.7 (range 1.2–31.4; median 3.7) at 1 h p.i. and was 8.3 ± 8.9 (range 1.1–46.9; median 4.5) at 3 h p.i.. SUVmax was 12.5 ± 13.2 (range 1.8–56.3; median 6.7) at 1 h p.i. and 15.8 ± 17.0 (range 2–82.5; median 9) at 3 h p.i.

SUVmean of lesions suggestive for LN metastases clearly (> 10%) increased in 65 lesions (71.4%), clearly decreased in ten lesions (11.0%), and remained stable in 16 (17.6%) of the lesions between 1 and 3 h p.i.

SUVmax of lesions suggestive for LN metastases clearly increased in 70 lesions (76.9%), clearly decreased in 13 lesions (14.3%), and remained stable in eight (8.8%) of the lesions between 1 and 3 h p.i.

SUV comparison

SUVmean and SUVmax were significantly higher in PSMA-positive mediastinal/paraaortal LN compared to PSMA-negative mediastinal/paraaortal LN at both imaging timings ($p < 0.001$ in all *t*-test comparisons in the mixed model).

SUVmean and SUVmax were also significantly higher in lesions suggestive for LN metastases of PC compared to mediastinal/paraaortal LN at both imaging timings ($p =$

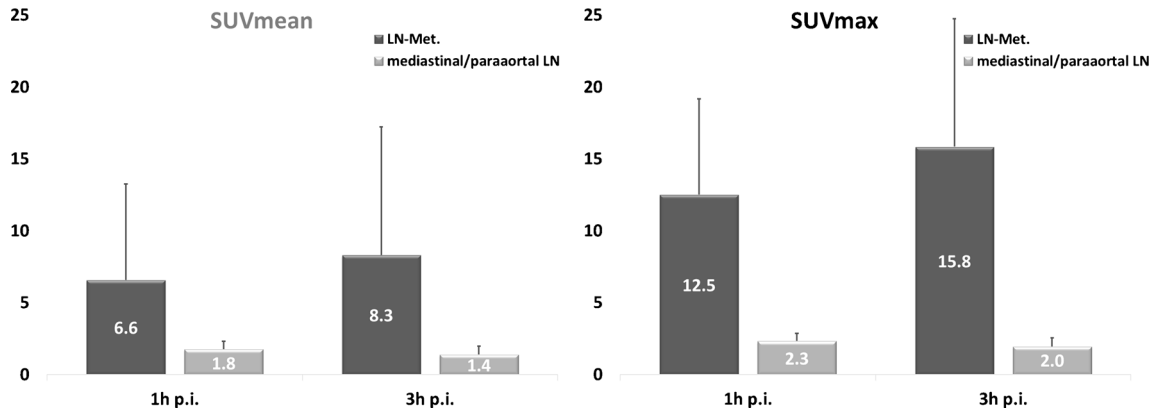

Fig. 6 SUVmean and SUVmax of both LN-metastases and PSMA-positive mediastinal/paraaortal LN at 1 h and 3 h p.i. As demonstrated by the figure, SUV of LN-metastases usually increase over time while SUV of mediastinal/paraaortal, PSMA-positive LN decrease

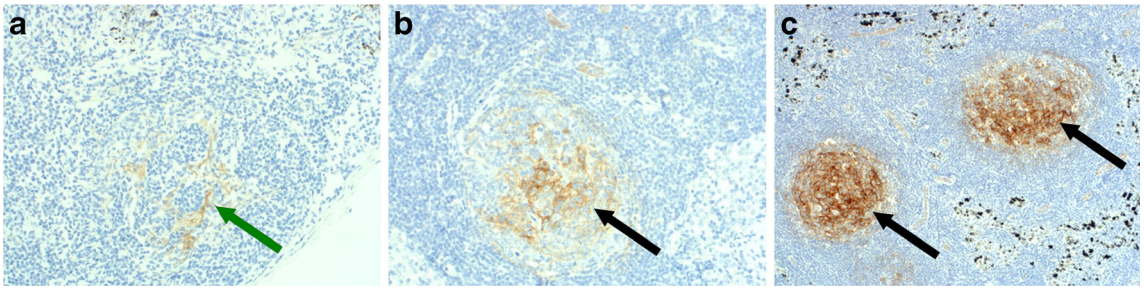

Fig. 7 All mediastinal lymph nodes analyzed in the current manuscript displayed PSMA expression in endothelial cells of small intranodal vessels with variable intensity (**a** weak expression in endothelial cells of a small intranodal vessel (*green arrow*) without expression in the adjacent lymphatic tissue elements). Expression of PSMA (**b**: moderate, **c**: strong) was observed in germinal centers (*black arrows*) of 68.1% of mediastinal lymph nodes analyzed in the current manuscript. Magnification: 100×

0.034 and $p = 0.026$ for SUVmax at 1 h and 3 h, and $p = 0.051$ and 0.035 for SUVmean at 1 h and 3 h: < 0.02 in all *t*-tests).

Histopathology

An overall of 22 lymph node groups were evaluated for PSMA expression by immunohistochemistry. Of these lymph node groups 11 were from the mediastinum, 11 were from paraaortal locations.

In the histopathological evaluation five lymph node groups showed extensive follicular hyperplasia and seven lymph node groups had focal follicular hyperplasia. All 11 mediastinal but no paraaortal lymph node groups had anthracosis. Three lymph nodes groups had fibrosis, one with calcification. The remaining seven lymph node groups had no pathological alteration (apart from anthracosis in those cases from the mediastinum).

As demonstrated by Figs. 7 and 8, expression of PSMA was found in intranodal endothelial cells of vessel walls as well as in lymphatic germinal centers to varying degrees. Expression in endothelial cells varied from weak to strong, 13 cases (59.2%) had weak expression, five (22.7%) had moderate expression, and four cases (18.2%) were strongly positive in endothelial cells. Seven cases (31.9%) had no positive germinal centers, five cases (22.7%) each had weak, moderate, and strongly positive germinal centers respectively.

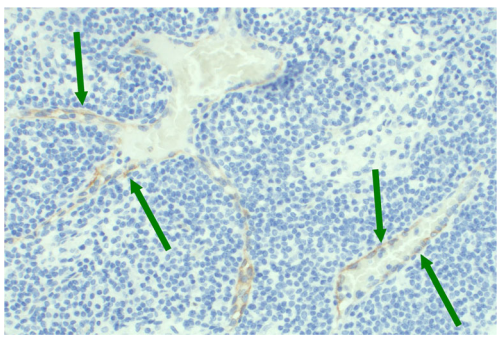

Fig. 8 Weak PSMA expression in endothelial cells of small intranodal vessels (*green arrows*). Magnification: 200×

When positivity for PSMA was correlated with pathology (Wilcoxon's test), we found no difference in regard to association of PSMA expression in vessel walls with and without morphological alterations ($p = 0.717$). In contrast, while PSMA expression in germinal center structures — as expected — was low in lymph nodes with fibrosis (mean rank: 7.67) and no pathology (mean rank: 7.29), cases with focal (mean rank: 15.0) and diffuse (mean rank: 14.8) follicular hyperplasia showed elevated PSMA expression levels ($p = 0.050$) indicating that non-specifically activated lymph nodes had an overall increased expression level of the protein. PSMA positivity in germinal centers varied depending on correlation with location (Wilcoxon's test). Mediastinal lymph nodes (mean rank: 14.28) showed significantly higher PSMA levels, and were thus significantly more likely to be positive than paraaortal (mean rank: 8.73) lymph nodes ($p = 0.038$). Vessel positivity was not correlated with site ($p = 1.0$). Although follicular hyperplasia (as a reason for a higher number of germinal centers) was slightly more frequent in mediastinal nodes (seven out of 11 cases, 63.6%) than in paraaortal nodes (five out of 11, 45.5%), the association was not significant (Fisher's exact test, $p = 0.67$) and could thereby not fully explain the significantly higher rate of positivity for PSMA in mediastinal nodes.

Discussion

The biodistribution of PSMA ligands shows physiological uptake in the lacrimal and salivary glands, in the liver, in the spleen, in the kidneys, in some parts of the intestines, and in coeliac ganglia, as described previously [5, 14]. The results of the current analysis confirmed our impression that a notable proportion of patients also present with PSMA-positive mediastinal/paraaortal LN: 18.4% of the patients presented with at least one PSMA-positive mediastinal LN at 1 h p.i., and 7.9% of the patients at 3 h p.i..

Initially, we speculated that the tracer may be accumulated within the mediastinal LN via the lymphatic system of the lungs. However, immunohistochemical analyses revealed a

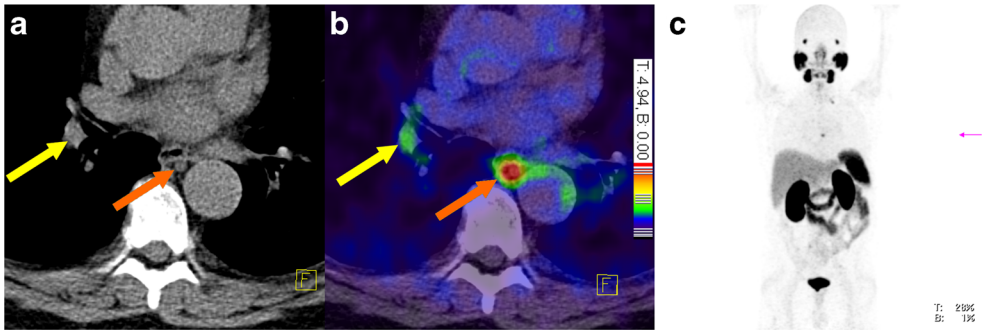

Fig. 9 Usually, PSMA-positive mediastinal/paraaortal LN (*yellow arrows*) can be easily distinguished from LN-metastases of PC (*orange arrows*) due to their significantly lower tracer uptake. **a** low-dose CT at 1 h p.i. **b** fusion of PET and CT at 1 h p.i. **c** Maximum intensity projection of PET at 1 h p.i.. Color scales as automatically produced by the PET/CT scanner

PSMA expression in intranodal vascular endothelia of all 22 randomly selected mediastinal and paraaortal LN of patients without PC history. In addition, PSMA expression was also present at differing degrees within germinal centers of 68.1% of the 22 above-mentioned LN groups. In this context, the question arises as to which of these LN would more likely present with a noticeable PSMA-ligand uptake in PET/CT. At this stage, we speculate that LN with follicular hyperplasia would more likely be visible in PSMA-ligand PET/CT, as they presented with the strongest PSMA expression. This constellation does not need to be limited to mediastinal/paraaortal LN. We assume that in all body locations, activation of LN could lead to PSMA-positive LN. However, it is obvious that mediastinal LN are frequently activated, as they are often

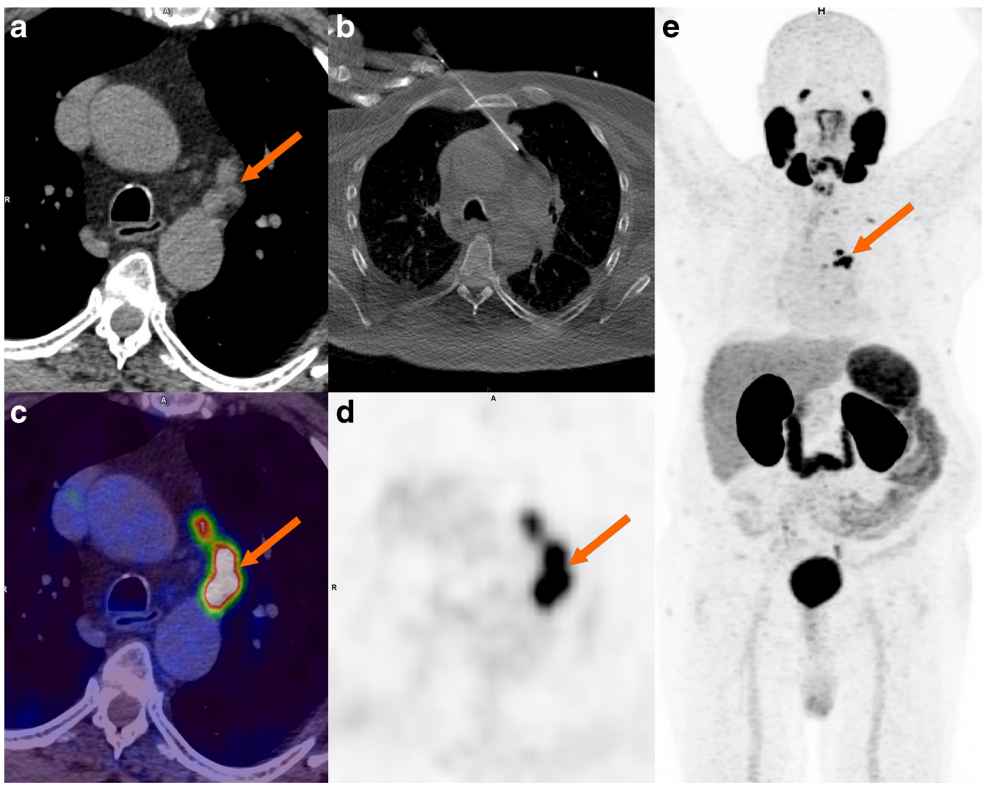

Fig. 10 This figure presents a rare case of histologically proven mediastinal LN-metastases of PC without evidence of other LN metastases caudal of them in ^{68}Ga-PSMA-11 PET/CT. The patient was pretreated in 2013 by radical prostatectomy (Gleason Score 9) followed by external beam radiation therapy. None of the 13 pelvic LN removed during the surgery were metastatic. However, in 2016 he was referred to ^{68}Ga-PSMA-11 PET/CT due to a biochemical relapse. As visible by the figure, several paraaortic lesions suggestive of LN-metastases of PC were detected (SUVmean 11.5; SUVmax 17.9). A subsequent CT-guided biopsy (**b**) proved mediastinal LN metastases of PC. This case was kindly provided by the Hospital Israelita Albert Einstein, São Paulo, Brazil. The patient was therefore not included in the patients' collective of the current study. **a** Low-dose CT of the PET/CT. **c** Fusion of PET and CT. **d** PET of the PET/CT. **e** Maximum intensity projection of the PET/CT

exposed to inflammatory processes derived from the lungs. At this stage, we could not find any information either about the reasons of PSMA expression in LN, or about the function of this receptor in activated lymphatic cells or vessel walls.

Usually, the PSMA-positive mediastinal/paraaortal LN show a low uptake as presented by Figs. 2, 3, 4, and 5. Indeed, the quantitative analyses revealed that PSMA-positive mediastinal/paraaortal LN show significantly lower tracer uptake compared to LN metastases. Therefore, it should be relatively easy to distinguish them from LN metastases, as demonstrated by Fig. 9. However, there exists a slight overlap of SUVs between the two LN types. In doubtful cases, the authors recommend conducting additional late scans: while the majority of LN metastases present with increasing tracer uptake over time — which is in line with previously published data [5, 15, 17–21] — the majority of mediastinal/paraaortal LN demonstrate the opposite. In addition, our results show that the patients usually presented with solely one PSMA-positive mediastinal/paraaortal LN. None of the patients had more than two PSMA-positive mediastinal/paraaortal LN. Contrarily, LN metastases, especially in more advanced disease, often present as a chain of clearly PSMA-positive lesions. This difference can also help to distinguish metastases from PSMA-positive LN of benign origin.

The overwhelming majority of PSMA-negative mediastinal/paraaortal LN presented with decreasing tracer uptake over time. This result is of low clinical relevance, was expected, and is in line with the background activity which is cleared by excretion via the urinary tract as demonstrated previously [5].

One limitation of the present analysis is the lack of systematic histological investigations of lesions suggestive of LN metastases of PC and PSMA-positive mediastinal/paraaortal LN respectively. However, especially with regard to PSMA-positive mediastinal/paraaortal LN, biopsy or resection is neither medically indicated nor ethically feasible. The strict selection criteria of group A minimize the risk of including patients with exclusively mediastinal/paraaortal LN metastases as presented by Fig. 10.

Due to the missing feasibility of a histological confirmation of the correct categorization (metastasis versus follicular hyperplasia) of PSMA-positive mediastinal/paraaortal LN, it would be inappropriate to provide SUV cut-offs for benign and malign LN. Therefore, the differentiation between the two LN types should be conducted according to the clinical context and the characteristics of both LN types described in this manuscript.

Overall, more studies are mandatory to further investigate the characteristics of activated LN in PSMA-ligand imaging. Until then, our results can potentially help to better distinguish between LN of benign origin and LN metastases of PC.

Conclusion

PSMA-positive mediastinal/paraaortal LN were visible in a notable proportion of patients. Subsequently, they should be regarded as a potential pitfall in image interpretation of PSMA-ligand PET/CT. PSMA expression in tumor-free mediastinal and paraaortal LN could be verified histologically. PSMA positivity on the histopathological level was associated with the activation state of such LN. Compared to LN suggestive for metastases of PC, mediastinal/paraaortal LN often occur isolated, and usually present with significantly lower tracer uptake, which, in addition, mostly decreases over time. In cases of uncertain grading of PSMA-positive LN, the authors therefore recommend conducting additional late scans (e.g., at 3 h p.i.): while the majority of LN metastases present with increasing tracer uptake over time, the majority of mediastinal/paraaortal LN demonstrate the opposite.

Acknowledgements A large number of people helped to plan, investigate, and analyze the patients in past years. Amongst them are (in alphabetic order): Heidrun Adam, Stephanie Biedenstein, Renate Brück, Elena Dahlke, Larissa Engel, Tanja Gerwert, Prof. Frederik Giesel, Daniela Johna, Dr. Christian Kleist, Dr. Susanne Krämer, Dr. Clemens Kratochwil, Kirsten Kunze, Viktoria Reiswich, Franziska Seybold-Epting, Peter Seybold-Epting, Fabian Spohn, and Natalia Zimmermann.

Compliance with ethical standards

Ethical approval All patients published in this manuscript signed a written informed consent form for the purpose of anonymized evaluation and publication of their data. All reported investigations were conducted in accordance with the Helsinki Declaration and with our national regulations (German Medicinal Products Act, AMG §13 2b). This evaluation was approved by the ethics committee of the University of Heidelberg (S-321-2012).

Conflicts of interest All authors declare that they have no conflict of interest.

References

1. Siegel R, Ma J, Zou Z, Jemal A. Cancer statistics. CA Cancer J Clin. 2014;64:9–29.
2. Israeli RS, Powell CT, Corr JG, Fair WR, Heston WD. Expression of the prostate-specific membrane antigen. Cancer Res. 1994;54:1807–11.
3. Maresca KP, Hillier SM, Femia FJ, Keith D, Barone C, Joyal JL, et al. A series of halogenated heterodimeric inhibitors of prostate specific membrane antigen (PSMA) as radiolabeled probes for targeting prostate cancer. J Med Chem. 2009;52:347–57.
4. Hillier SM, Maresca KP, Femia FJ, Marquis JC, Foss CA, Nguyen N, et al. Preclinical evaluation of novel glutamate–urea–lysine analogues that target prostate-specific membrane antigen as molecular imaging pharmaceuticals for prostate cancer. Cancer Res. 2009;69:6932–40.
5. Afshar-Oromieh A, Malcher A, Eder M, Eisenhut M, Linhart HG, Hadaschik BA, et al. PET imaging with a [68Ga]gallium-labelled PSMA-ligand for the diagnosis of prostate cancer: biodistribution in

humans and first evaluation of tumour lesions. Eur J Nucl Med Mol Imaging. 2013;40:486–95.

6. Afshar-Oromieh A, Zechmann CM, Malcher A, Eder M, Eisenhut M, Linhart HG, et al. Comparison of PET imaging with a (68)Ga-labelled PSMA-ligand and (18)F-choline-based PET/CT for the diagnosis of recurrent prostate cancer. Eur J Nucl Med Mol Imaging. 2014;41:11–20.
7. Afshar-Oromieh A, Avtzi E, Giesel FL, Holland-Letz T, Linhart HG, Eder M, et al. The diagnostic value of PET/CT imaging with the (68)Ga-labelled PSMA-ligand HBED-CC in the diagnosis of recurrent prostate cancer. Eur J Nucl Med Mol Imaging. 2015;42: 197–209.
8. Eiber M, Maurer T, Souvatzoglou M, Beer AJ, Ruffani A, Haller B, et al. Evaluation of hybrid ^{68}Ga-PSMA-ligand PET/CT in 248 patients with biochemical recurrence after radical prostatectomy. J Nucl Med. 2015;56:668–74.
9. Afshar-Oromieh A, Holland-Letz T, Giesel FL, Kratochwil C, Mier W, Haufe S, et al. Diagnostic performance of (68)Ga-PSMA-11 (HBED-CC) PET/CT in patients with recurrent prostate cancer: evaluation in 1007 patients. Eur J Nucl Med Mol Imaging. 2017: 44(8):1258–68.
10. Zechmann CM, Afshar-Oromieh A, Armor T, Stubbs JB, Mier W, Hadaschik B, et al. Radiation dosimetry and first therapy results with a (124)I/ (131)I-labeled small molecule (MIP-1095) targeting PSMA for prostate cancer therapy. Eur J Nucl Med Mol Imaging. 2014;41:1280–92.
11. Afshar-Oromieh A, Haberkorn U, Zechmann C, Armor T, Mier W, Spohn F, et al. Repeated PSMA-targeting radioligand therapy of metastatic prostate cancer with (131)I-MIP-1095. Eur J Nucl Med Mol Imaging. 2017;44:950–9.
12. Chang SS. Overview of prostate-specific membrane antigen. Rev Urol. 2004;6(Suppl 10):S13–8.
13. Sheikhbahaei S, Afshar-Oromieh A, Eiber M, Solnes LB, Javadi MS, Ross AE, et al. Pearls and pitfalls in clinical interpretation of prostate-specific membrane antigen (PSMA)-targeted PET imaging. Eur J Nucl Med Mol Imaging. 2017;44(12):2117–36
14. Krohn T, Verburg FA, Pufe T, Neuhuber W, Vogg A, Heinzel A, et al. 68Ga-PSMA-HBED uptake mimicking lymph node metastasis in coeliac ganglia: an important pitfall in clinical practice. Eur J Nucl Med Mol Imaging. 2015;42:210–4.
15. Afshar-Oromieh A, Hetzheim H, Kübler W, Kratochwil C, Giesel FL, Hope TA, et al. Radiation dosimetry of (68)Ga-PSMA-11 (HBED-CC) and preliminary evaluation of optimal imaging timing. Eur J Nucl Med Mol Imaging. 2016;43:1611–20.
16. Eder M, Neels O, Müller M, Bauder-Wüst U, Remde Y, Schäfer M, et al. Novel preclinical and radiopharmaceutical aspects of [68Ga]Ga-PSMA-HBED-CC: a new PET tracer for imaging of prostate cancer. Pharm Basel Switz. 2014;7:779–96.
17. Herrmann K, Bluemel C, Weineisen M, Schottelius M, Wester H-J, Czernin J, et al. Biodistribution and radiation dosimetry for a probe targeting prostate-specific membrane antigen for imaging and therapy. J Nucl Med. 2015;56:855–61.
18. Afshar-Oromieh A, Hetzheim H, Kratochwil C, Benesova M, Eder M, Neels OC, et al. The theranostic PSMA-ligand PSMA-617 in the diagnosis of prostate cancer by PET/CT: biodistribution in humans, radiation dosimetry, and first evaluation of tumor lesions. J Nucl Med. 2015;56:1697–705.
19. Afshar-Oromieh A, Sattler LP, Mier W, Hadaschik B, Debus J, Holland-Letz T, et al. The clinical impact of additional late PET/CT imaging with 68Ga-PSMA-11 (HBED-CC) in the diagnosis of prostate cancer. J Nucl Med. 2017;58(5):750–755
20. Sahlmann C-O, Meller B, Bouter C, Ritter CO, Ströbel P, Lotz J, et al. Biphasic ^{68}Ga-PSMA-HBED-CC-PET/CT in patients with recurrent and high-risk prostate carcinoma. Eur J Nucl Med Mol Imaging. 2016;43:898–905.
21. Wondergem M, van der Zant F, Knol R, Lazarenko S, Pruim J, de Jong IJ. 18F-DCFPyL PET/CT in the detection of prostate cancer at 60 and 120 minutes; detection rate, image quality, activity kinetics and biodistribution. J Nucl Med. 2017;58(11):1797–1804